Spin Frustrated Pyrazolato Triangular CuII Complex. Structure and Magnetic Properties, an Overview.

Walter Cañón-Mancisidor *, Patricio Hermosilla-Ibáñez, Evgenia Spodine *, Verónica Paredes-García, Carlos J. Gómez-García, Diego Venegas-Yazigi *

Posted Date: 25 May 2023

doi: 10.20944/preprints202305.1726.v1

Keywords: Cu3-□3OH complex; pyrazolato ligands; trinuclear complex; Spin Frustration; magnetic susceptibility; antisymmetric exchange; DFT calculations.

Article

Spin Frustrated Pyrazolato Triangular Cu^{II} Complex. Structure and Magnetic Properties, an Overview

Walter Cañón-Mancisidor [1,4,*], Patricio Hermosilla-Ibáñez [2,3], Evgenia Spodine [2,4,*], Verónica Paredes-García [2,5], Carlos J. Gómez-García [6] and ego Venegas-Yazigi [2,3,*]

[1] Depto. Matemáticas y Ciencias de la Ingeniería (DMCI), Facultad de Ingeniería, Ciencia y tecnología (FICyT), Universidad Bernardo O'Higgins (UBO), Av. Viel 1497, Santiago, Chile, CP-8370993; walter.canon@ubo.cl (W.C.-M).

[2] Centro para el Desarrollo de la Nanociencia y Nanotecnología, (CEDENNA), USACH, Av. Lib. Bernardo O´Higgins 3363, Estación Central, Chile, CP-9170022.

[3] Depto. Química de los Materiales, Facultad de Química y Biología, Universidad de Santiago de Chile (USACH), Av. Lib Bernardo O´Higgins 3363, Estación Central, Chile, CP-9170022; patricio.hermosilla@usach.cl (P.H.-I); diego.venegas@usach.cl (D.V.-Y.).

[4] Facultad de Ciencias Químicas y Farmacéuticas, Universidad de Chile, Dr. Carlos Lorca Tobar 964, Independencia, Chile, CP-8380000; espodine@uchile.cl (E.S.).

[5] Departamento de Ciencias Químicas, Universidad Andrés Bello, Republica 275, Santiago, Chile, CP-8370146; vparedes@unab.cl (V.P.-G).

[6] Departamento de Química Inorgánica, Universidad de Valencia, C/Dr. Moliner 50, Burjasot, Valencia, Spain, CP-46100; carlos.gomez@uv.es (C.J.G.-G).

* Correspondence: walter.canon@ubo.cl (W.C.-M); diego.venegas@usach.cl (D.V.-Y.); espodine@uchile.cl (E.S.).

Abstract: The synthesis and structural characterization of a new triangular Cu_3-μ_3OH pyrazolato complex of formula, $[Cu_3(\mu_3\text{-}OH)(pz)_3(Hpz)_3][BF_4]_2$ (**1-Cu$_3$**), Hpz = pyrazole, is presented. The triangular unit forms a quasi-isosceles triangle with Cu-Cu distances of 3.3739(9), 3.3571(9), and 3.370(1) Å. This complex is isostructural to the hexanuclear complex $[Cu_3(\mu_3\text{-}OH)(pz)_3(Hpz)_3](ClO_4)_2]_2$ (**QOPJIP**). A comparative structural analysis with other reported triangular Cu_3-μ_3OH pyrazolato complexes has been done, showing that, depending on the pyrazolato derivative, auxiliary ligand or counter-anion can affect the nuclearity and/or the dimensionality of the system. The magnetic properties of **1-Cu$_3$** are analyzed by experimental data and DFT calculation. A detailed analysis is done on the magnetic properties comparing experimental and theoretical data of other molecular triangular Cu_3-μ_3OH complexes, showing that the displacement of the μ_3-OH^- from the Cu_3 plane, together with the type of organic ligands, influences the nature of the magnetic exchange interaction between the spin-carrier centers, since it affects the overlap of the magnetic orbitals involved in the exchange pathways. Finally, a detailed comparison of the magnetic properties of **1-Cu$_3$** and **QOPJIP** was done, which allowed us to understand the differences in their magnetic properties.

Keywords: Cu_3-μ_3OH complex; pyrazolato ligands; trinuclear complex; Spin Frustration; magnetic susceptibility; antisymmetric exchange; DFT calculations

1. Introduction

Triangular Cu^{II} complexes have been largely studied in the literature, and among them, several systems present a μ_3-X^- (X = Cl^-, Br^-, OH^-, O^{2-}) bridging unit that, together with other organic auxiliary ligands enables to obtain very stable systems [1–3]. Due to their high stability, these triangular fragments can be used as secondary building units (SBU) in constructing several coordination polymers or MOFs systems [4–6].

Moreover, triangular complexes are an interesting class of materials since they have been suggested as possible qubits, as they can present spin-electron coupling due to the interplay between three main factors (spin exchange, spin-orbit interaction, and chirality) [7–12]. Spin Frustration (SF) has been suggested as the origin of the abovementioned features. This phenomenon originates when

 doi:10.20944/preprints202305.1726.v1

an odd number of non-integer spin carriers that are antiferromagnetically coupled cannot be satisfied simultaneously, like in a triangular system [13]. Thus, the energy of the ground state is doubly degenerate, but distortions of the C_3 symmetry of the triangle or by the antisymmetric exchange, which is related to spin-orbit interactions, can break this degeneracy by lowering the symmetry of the system [14,15].

These triangular Cu^{II} systems have been largely studied since they formed the simplest spin-triangle. This has allowed the possibility of studying in detail the magnetic properties of geometrically spin-frustrated systems [16]. Among these systems, the ones with a hydroxy bridge (μ_3-OH^-) are among the most reported in the literature [17,18]. Systems presenting pyrazolato, triazolato, and other types of auxiliary organic ligands have been magnetically studied in the literature [19,20]. In general, the displacement of the μ_3-OH^- from the Cu_3 plane, together with the type of organic ligands, have been related to the nature of the magnetic exchange interaction between the spin-carrier centers since they affect the overlap of the magnetic orbitals involved in the exchange pathways [21].

Among all the mentioned systems, Cu_3-μ_3OH pyrazolato complexes are among the most reported systems, and they present strong antiferromagnetic properties [22,23]. However, they have not been extensively analyzed in search of magneto-structural features, as has been done for the triazolato complexes [24]. These compounds, depending on the pyrazolato derivative, auxiliary ligand, or counter-anion, may present different nuclearity and/or dimensionality [3,19].

In this work, we present the synthesis and structural characterization of a triangular Cu_3-μ_3OH pyrazolato complex of formula, $[Cu_3(\mu_3\text{-}OH)(pz)_3(Hpz)_3][BF_4]_2$ (**1-Cu$_3$**), Hpz = pyrazole. Interestingly, this trinuclear complex is isostructural to the hexanuclear **QOPJIP** structure $[Cu_3(\mu_3\text{-}OH)(pz)_3(Hpz)_3(ClO_4)_2]_2$, since the perchlorate anions connect the two triangular units [25]. An extensive structural analysis with other reported triangular Cu_3-μ_3OH pyrazolato complexes has been done. The magnetic properties of **1-Cu$_3$** are analyzed by experimental data together with DFT calculation, showing that strong antiferromagnetic interactions exist between the Cu^{II} centers. We present a detailed analysis of the magnetic properties of **1-Cu$_3$** and compare them with the experimental data of other molecular triangular Cu_3-μ_3OH pyrazolato complexes and with the theoretical magnetic properties of a previously reported Cu_3-μ_3OH complex [21]. Finally, we perform a detailed study of the magnetic properties of **1-Cu$_3$** and **QOPJIP** to understand the differences in their magnetic properties.

2. Results and Discussion

ESI-Mass and FTIR Spectra

ES-MS in positive mode (acetonitrile) shows the existence of different fragments of the $[Cu_3\text{-}\mu_3OH]^{n+}$ unit, such as: $\{[Cu_3(\mu_3\text{-}OH)(pz)_3(Hpz)_3][BF_4]\}^+$ (m/Z = 700); $\{[Cu_3(\mu_3\text{-}OH)(pz)_3(Hpz)_3]+1e^-\}^+$ (m/Z = 613); $\{[Cu_3(\mu_3\text{-}OH)(pz)_3(Hpz)_2]+1e^-\}^+$ (m/Z = 544); $\{[Cu_3(\mu_3\text{-}OH)(pz)_3(Hpz)_1]\ ]+1e^-\}^+$ (m/Z = 476) and $\{[Cu_3(\mu_3\text{-}OH)(pz)_3\}^+$ (m/Z = 408). See Figure S1. Complementary analyses (EA and FTIR spectroscopy) confirm the purity of the crystalline material (see supporting information, section S2, FTIR).

Structure Analysis

The triangular complex (**1-Cu$_3$**) crystallizes in the centrosymmetric monoclinic space group $P2_1/c$ (For more information, see CIF file and section S3). The molecular structure consists of a triangular $[Cu_3\text{-}\mu_3OH]^{n+}$ core surrounded by three protonated Hpz and three deprotonated pz^- ligands, forming the cationic complex $[Cu_3(\mu_3\text{-}OH)(pz)_3(Hpz)_3]^{2+}$, which is counterbalanced by two tetrafluoroborate anions. The trinuclear unit is formed by two Cu^{II} (Cu1 and Cu3) centers with a square pyramid (SqP) geometry and an octahedral Cu2 center (O_h) with a Jahn-Teller distortion. This triangular unit presents pseudo-three-fold symmetry forming an isosceles triangle, with copper-copper distances of 3.3740(8), 3.3574(8), and 3.3702(8) Å for Cu1-Cu2, Cu2-Cu3, and Cu1-Cu3, respectively. As observed for similar systems, the μ_3-OH^- group is not coplanar with the plane formed by the three copper

 doi:10.20944/preprints202305.1726.v1

centers, displaced by 0.439 Å. Other displacements reported in the literature for the $[Cu_3\text{-}\mu_3OH]^{n+}$ are in the range of 0.363 and 0.759 Å [23,26]. The metal centers present three different types of Cu-O, Cu-N, and Cu-F bonds. The first is around 2.00 Å, the second is between 1.98 and 2.02 Å, and the third is between 2.48 and 2.58 Å (Figure 1).

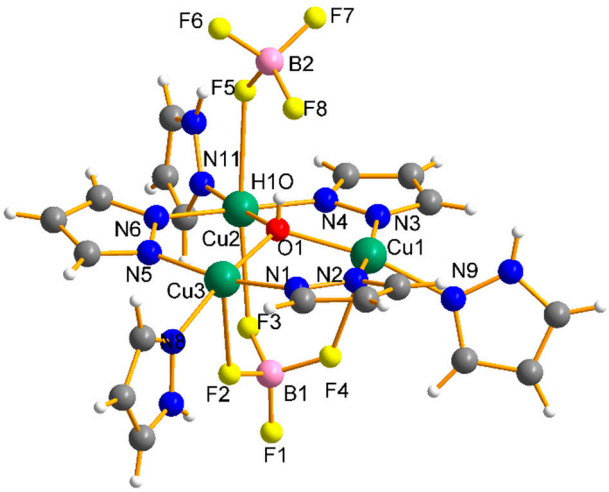

Figure 1. Crystal structure of the triangular complex $[Cu_3(\mu_3\text{-}OH)(pz)_3(Hpz)_3][BF_4]_2$ (**1-Cu$_3$**), Color code: Cu = green, O = red, N = blue, C = grey, H = white, B = light pink and F = light yellow.

An original aspect of **1-Cu$_3$** is the presence of two $[BF_4]^-$ counter-anions (B1 and B2) coordinated to the copper centers of the trinuclear unit. In fact, **1-Cu$_3$** is the first example of a triangular pyrazolato complex with this type of counter-anion. One of the $[BF_4]^-$ anions (B1) presents a μ_3 coordination mode with three F atoms coordinated to the three Cu^{II} centers (with F-Cu distances of 2.483(3), 2.530(4), and 2.581(4) Å). The other $[BF_4]^-$ anion (B2) is only coordinated by one F atom to a single Cu^{II} center (Cu2-F5 = 2.557(4) Å). The structure presents an inversion center (outside the complex) that generates a second triangular $[Cu_3(\mu_3\text{-}OH)(pz)_3(Hpz)_3][BF_4]_2$ unit, where the fluorine atom (F7) of the $[BF_4]^-$ anion (B2) is semi-coordinated to Cu1 with a long distance of 2.812(3) Å. Finally, it is worth mentioning that between the triangular units, there are some hydrogen bonds that stabilize the crystal lattice of the complex, with inter-cluster Cu···Cu distances ranging between 7.309(1) and 13.4522(9) Å (Figure 2).

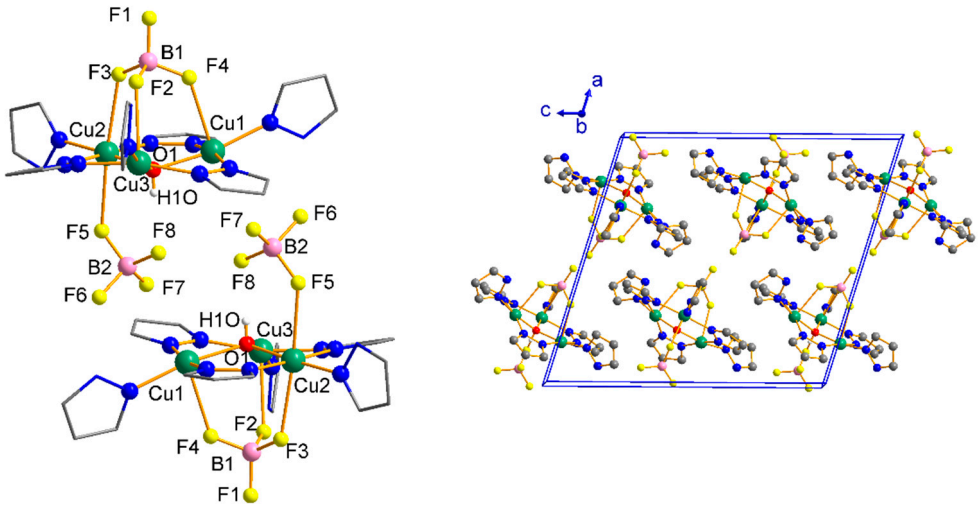

Figure 2. Crystal packing of the triangular complex $[Cu_3(\mu_3\text{-}OH)(pz)_3(Hpz)_3][BF_4]_2$ (**1-Cu$_3$**), Color code: Cu = green, O = red, N = blue, C = grey, H = white, B = light pink and F = light yellow.

 doi:10.20944/preprints202305.1726.v1

According to the CCDC database, there are at least 96 structures based on pyrazolato (R-pz$^-$) ligands, forming complexes with the general formula $[Cu_3(\mu_3\text{-}OH)(R\text{-}pz)_3(L)_3]^{n+/-}$, where R = -H, -$CH_3$, -$NO_2$, among others, and L = $pz^{0/-}$, Cl^-, H_2O, NO_3^-,… [2,6,22,23,25–30]. The nature of the axial ligand and the type of substitution of the pz$^-$ ligand leads to the formation of either high dimensional systems (usually for R = -COO^-) or discrete complexes. If the axial ligand is monodentate or acts as a chelate or if the pz- ligand's substituent group cannot coordinate with other metal centers, discrete (0D) systems are formed, see Table 1. As a general trend, we observe that when larger ligands are present either as axial or auxiliar ligands, the distance between the Cu_3 plane and the μ_3-OH^- group increases. We also observe that when auxiliary ligands are present, the triangular units can form hexanuclear units by coordinating these auxiliar ligands to the metal centers of the closest triangular units (**RUYGEX**, **RUYGIB**, **RUYHEY**, **RETQUD**, **QOPJIP, DIBXOC, EGIXUQ, EHOLIZ**).

Among the compounds of Table 1, **QOPJIP**: $[Cu_3(\mu_3\text{-}OH)(pz)_3(Hpz)_3][ClO_4]_2$) [25] is isostructural to **1-Cu$_3$** ($[Cu_3(\mu_3\text{-}OH)(pz)_3(Hpz)_3][BF_4]_2$), although there are some differences, mainly related to the nature of the counter-anion. The smaller size of the $[BF_4]^-$ unit located between the two triangular units (compared to ClO_4^-) leads to an important shortening of the distances between the Cu_3-planes for **1-Cu$_3$** (6.789 Å) as compared to **QOPJIP** (7.044 Å). This shortening allows the formation of a hydrogen bond between F8 and the hydrogen atom of the μ_3-OH group (not observed in **QOPJIP**), enlarging the O-H bond in **1-Cu$_3$** (0.991 Å), compared to **QOPJIP** (0.979 Å). The lower coordination capacity of BF_4^- compared to ClO_4^- is clearly observed in **1-Cu$_3$**, where the $Cu_3(\mu_3$-OH) units are isolated (except for a very long semi-coordinated Cu1-F7 bond of 2.811(3) Å). In contrast, in **QOPJIP,** the ClO_4^- anion connects two triangular Cu_3 units through four short Cu-O bonds (in the range 2.44-2.66 Å) to form a hexanuclear complex.

Table 1. Structural parameters of triangular Cu_3 systems of the type $[Cu_3(\mu_3\text{-}OH)(R\text{-}pz)_3(L)_3]^{n+/-}$.

CCDC Code	Cu^{II}-Cu^{II} (Å)	Cu_3(plane)-OH (Å)	Cu_n-OH (Å)	Cu_n-N(pz) (Å)	Cu_{n-1}-Cu_n-Cu_{n+1} (º)	Cu_n-OH-Cu_{n+1} (º)	Ref.
1-Cu$_3$	3.3740(8) 3.3574(8) 3.3702(9)	0.439	2.005(3) 1.978(3) 1.995(3)	1.942(4) to 1.965(3)	59.71(2) 60.09(2) 60.20(2)	115.8(2) 115.3(2) 114.8(2)	This work
AMACIC	3.3020(6) 3.2561(5) 3.3927(6)	0.553	1.977(2) 2.001(2) 2.005(2)	1.932(3) to 1.947(2)	58.19(1) 62.30(1) 59.51(1)	112.20(9) 116.9(1) 108.73(9)	[27]
ASUNIN	3.3456(1) 3.3266(6) 3.3456(1)	0.510	2.011(1) 1.932(5) 2.042(5)	1.918(3) to 1.952(1)	59.62(1) 60.19(1) 60.19(1)	116.1(1) 113.6(2) 111.3(1)	[28]
BOFLEP	3.349(2) 3.239(2) 3.355(2)	0.580	2.005(4) 2.001(4) 1.995(3)	1.924(5) to 1.958(4)	57.78(2) 61.20(2) 61.02(2)	113.5(2) 108.3(2) 114.1(2)	[29]
DEFSEN	3.384(1) 3.2503(9) 3.2950(9)	0.567	1.975(3) 2.008(3) 2.000(2)	1.928(4) to 1.948(4)	58.22(2) 59.52(2) 62.26(2)	116.3(1) 108.4(1) 112.0(1)	[22]
DIBXOC	3.2972(5) 3.2972(5) 3.3843(4)	0.609	2.008(2) 2.030(2) 2.008(2)	1.946(2) to 1.1.957	59.12(1) 61.76(1) 59.12(1)	109.5(1) 109.5(1) 114.9(1)	[31]
EGIXOK	3.3540(5) 3.3874(6) 3.4036(6)	0.363	1.979(2) 1.993(2) 1.985(3)	1.921(3) to 1.941(2)	60.16(1) 60.64(1) 59.19(1)	115.2(2) 116.7(2) 118.3(2)	[26]
EGIXUQ	3.268(1) 3.379(1) 3.350(1)	0.148	1.936(5) 1.943(4) 1.913(5)	1.914(5) to 1.942(5)	61.39(2) 60.50(2) 58.11(2)	114.8(2) 121.0(2) 122.4(2)	[26]
EHOLIZ	3.389(5) 3.389(5) 3.389(5)	0.274	2.046(10) 1.941(10) 1.941(10)	1.92(1) to 1.97(2)	60.0(1) 60.0(1) 60.0(1)	116(1) 122(1) 116(1)	[32]

 doi:10.20944/preprints202305.1726.v1

JEWWEO	3.3416(8) 3.3825(8) 3.3502(7)	0.461	1.988(3) 2.010(3) 1.982(3)	1.923(4) to 1.943(4)	60.73(2) 59.76(2) 59.51(2)	113.4(1) 115.9(2) 115.1(2)	[2]
JEWWIS	3.387(1) 3.309(1) 3.350(1)	0.486	1.976(6) 2.021(5) 1.985(6)	1.919(7) to 1.952(8)	58.84(3) 60.03(3) 61.13(3)	115.9(3) 111.4(3) 115.5(3)	[2]
MUZQUU	3.3696(5) 3.3461(5) 3.3788(5)	0.455	1.982(2) 2.003(2) 2.001(2)	1.947(3) to 1.960(2)	59.45(1) 60.41(1) 60.14(1)	115.45(9) 113.39(9) 116.05(9)	[6]
***QIMSIQ-a**	3.2977(4) 3.1704(4) 3.3126(4)	0.688	2.016(2) 2.012(2) 1.987(2)	1.938(2) to 1.959(2)	57.32(1) 61.58(1) 61.10(1)	109.91(7) 104.90(7) 111.68(8)	[23]
***QIMSIQ-b**	3.3911(4) 3.3023(4) 3.3214(4)	0.512	2.000(1) 1.994(2) 1.989(2)	1.944(2) to 1.959(2)	58.93(1) 59.48(1) 61.59(1)	116.20(8) 111.99(7) 112.72(7)	[23]
***QIMSOW-a**	3.2559(7) 3.342(1) 3.2345(9)	0.713	1.992(3) 2.032(3) 2.044(3)	1.941(4) to 1.958(4)	61.98(2) 58.69(2) 59.32(2)	108.0(1) 110.2(1) 106.6)1)	[23]
***QIMSOW-b**	3.2045(6) 3.1837(8) 3.2007(9)	0.759	1.985(3) 2.011(2) 1.990(3)	1.948(3) to 1.960(4)	59.61(2) 60.13(2) 60.25(2)	106.6(1) 105.4(1) 107.3(1)	[23]
QOPJIP	3.355(1) 3.386(1) 3.368(1)	0.466	1.994(5) 2.000(4) 2.007(5)	1.929(6) to 1.958(6)	59.94(3) 60.49(3) 59.57(3)	114.3(2) 114.4(2) 115.6(2)	[25]
QUSMEX	3.344(2) 3.286(2) 3.392(2)	0.475	1.955(8) 2.017(6) 1.992(9)	1.933(9) to 1.978(9)	58.39(4) 61.53(4) 60.07(4)	114.7(4) 110.1(4) 118.5(4)	[30]
QUSMIB	3.289(2) 3.289(2) 3.289(2)	0.489	1.961(1) 1.962(1) 1.960(1)	1.89(1) to 1.930(8)	60.00(4) 60.00(4) 60.00(4)	114.0(1) 114.0(1) 114.0(1)	[30]
QUSMUN	3.3550(5) 3.3615(5) 3.3439(6)	0.471	1.985(2) 2.005(2) 1.987(2)	1.937(2) to 1.951(2)	60.24(1) 59.72(1) 60.04(1)	114.42(9) 114.68(9) 114.65(9)	[30]
RETQUD	3.3833(6) 3.3629(6) 3.3769(5)	0.542	2.026(2) 2.028(3) 2.013(2)	1.942(3) to 1.961(2)	59.66(1) 60.07(1) 60.26(1)	113.1(1) 112.7(1) 113.5(1)	[19]
RETRAK	3.365(1) 3.3650(9) 3.3886(8)	0.565	2.023(3) 2.041(3) 2.019(2)	1.933(3) to 1.962(5)	59.77(2) 60.46(2) 59.77(2)	111.8(1) 111.9(1) 113.9(1)	[19]
RETREO	3.3442(6) 3.3975(6) 3.3022(7)	0.625	2.024(2) 2.033(2) 2.038(2)	1.936(3) to 1.957(3)	61.48(1) 58.65(1) 59.87(1)	111.0(1) 113.1(1) 108.7(1)	[19]
RUYGEX	3.4471(9) 3.206(1) 3.4227(9)	0.524	1.987(3) 2.024(3) 2.035(3)	1.940(4) to 1.953(4)	55.55(2) 62.01(2) 62.44(2)	118.5(1) 104.4(1) 117.3(1)	[3]
RUYGIB	3.2473(8) 3.4007(6) 3.4305(8)	0.507	2.014(3) 2.017(2) 1.989(2)	1.933(4) to 1.952(4)	61.16(1) 62.08(1) 56.76(1)	107.3(1) 116.2(1) 118.0(1)	[3]
RUYHEY	3.414(1) 3.253(1) 3.277(1)	0.613	2.012(5) 2.006(4) 2.016(3)	1.929(7) to 1.950(5)	58.15(3) 58.82(3) 63.03(3)	116.4(2) 108.0(2) 108.9(2)	[3]
SIJKOL	3.112(1) 3.321(1) 3.321(1)	0.658	2.000(1) 2.000(1) 1.977(1)	1.942(1) to 1.967(4)	62.06(1) 62.06(1) 55.88(1)	102.2(1) 113.3(1) 113.3(1)	[33]

Preprints.org (www.preprints.org) | NOT PEER-REVIEWED | Posted: 25 May 2023 doi:10.20944/preprints202305.1726.v1

UZIWEI	3.3695(6) 3.2840(5) 3.2953(5)	0.595	1.998(2) 2.004(2) 2.104(2)	1.937(2) to 1.952(2)	59.03(1) 59.36(1) 61.61(1)	114.68(8) 109.64(8) 110.42(8)	[34]
VAZCOR	3.1913(9) 3.391(1) 3.353(1)	0.599	2.032(4) 2.030(4) 1.959(3)	1.933(6) to 1.960(5)	62.36(2) 61.16(2) 56.49(2)	103.6(2) 116.4(2) 114.3(2)	[35]
VIMYEX	3.2639(7) 3.1851(8) 3.299(1)	0.712	2.027(2) 1.991(2) 2.003(2)	1.935(2) to 1.950(2)	58.06(1) 61.52(1) 60.41(1)	108.67(7) 105.79(7) 109.9387)	[36]
XOKXAX	3.347(1) 3.403(1) 3.320(1)	0.491	1.998(4) 2.000(4) 2.000(4)	1.939(5) to 1.963(6)	61.38(2) 58.92(2) 59.70(2)	113.6(2) 116.6(2) 112.3(2)	[37]
YIFGIG	3.3500(8) 3.2440(7) 3.3519(6)	0.521	1.978(2) 1.968(2) 2.008(2)	1.928(2) to 1.953(2)	57.90(1) 61.08(1) 61.02(1)	116.20(9) 109.37(9) 114.48(9)	[17]

*In **QIMSIQ** and **QIMSOW,** the letters a and b denote the structure that presents two different triangular Cu_3 units.

Magnetic Properties. dc Magnetic Measurements

The thermal variation of the product of the molar magnetic susceptibility per Cu_3 unit, times the temperature for **1-Cu$_3$**, measured with a DC field of 100 mT, shows a value of around 0.5 cm^3 K mol^{-1} at 300 K (Figure 3). This value is below the expected one for three uncoupled paramagnetic Cu(II) ions (1.125 cm^3 K mol^{-1} with g = 2.0), indicating the existence of bulk antiferromagnetic interactions between the Cu^{II} atoms of the $Cu_3(\mu_3\text{-OH})$ core. When the temperature is lowered, χ_mT steadily decreases, reaching a plateau between 130 and 100 K. Below 100 K, χ_mT further decreases and reaches a value of 0.26 cm^3 K mol^{-1} at 2 K. The χ_mT value in the plateau is 0.38-0.40 cm^3 K mol^{-1}, which is the expected value for a trinuclear unit with an S = 1/2 ground state [24,25]. The field dependence of the magnetization at 2 K for **1-Cu$_3$** shows at 5 T a value of around 0.7 μ_B, corresponding to *ca.* 0.7 electrons, although saturation is not fully reached at 5 T (Figure 3). This behavior is typical of systems with a μ_3-hydroxido moiety with a ground state of S = 1/2 (M = 1 μ_B) that present magnetization values below the expected ones and do not reach saturation, even at high fields [17,35]. Comparing the experimental data with those calculated by the PHI program (see below) for **1-Cu$_3$** shows a good agreement between them. The lower values of the experimental data confirm the presence of antisymmetric exchange.

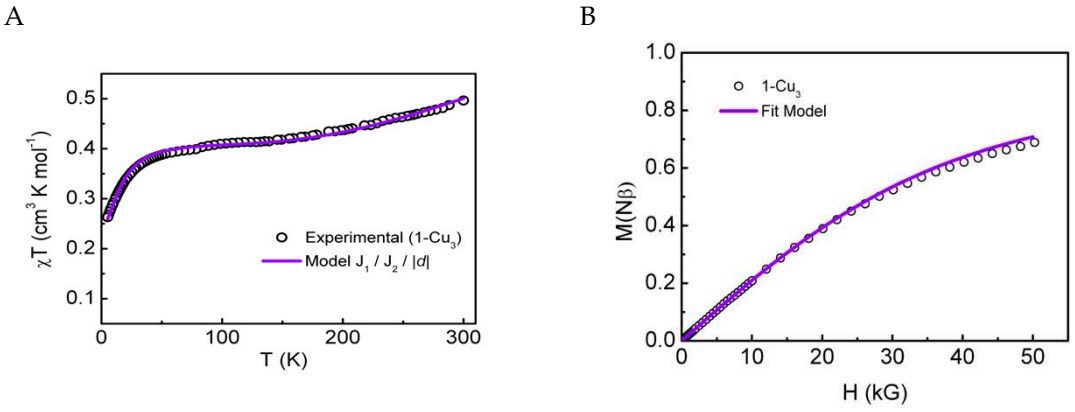

Figure 3. A. Thermal dependence of χ_mT for **1-Cu$_3$** at 100 mT. The solid line is the best fit obtained considering an isosceles triangle and the antisymmetric exchange; see equation 1 (PHI code). **B**. Experimental M(H) plot at 2 K for **1-Cu$_3$**, purple line - calculated magnetization curve using the PHI code.

 doi:10.20944/preprints202305.1726.v1

The magnetic behavior observed at low temperatures for the χT data can be associated with the spin frustration phenomena, which allows the existence of an antisymmetric exchange, as described by Ferrer *et al.*[24]. This work described in detail the antisymmetric exchange interaction in a triangular Cu_3 system based on triazolato derivatives. Additionally, we cannot discard that geometry distortions on the local coordination environment may influence the overall magnetic properties. In this sense, several discussions have arisen from this point, and according to Niedner-Schatteburg *et al.*, spin frustration leads to *geometric* distortion [38–40].

The fit of the *dc* experimental data was done using the PHI program [41]. At first, only the isotropic interactions for the triangular arrangement were considered, giving a good fit in the 50-300 K range. The best fit in the whole temperature range was obtained by adding to the model the antisymmetric exchange (ASE; G_{ij}), which is a non-isotropic interaction [15,24]. Thus, based on the structural arrangement of the Cu^{II} triangles, we have used a model with two isotropic exchange interactions (J_1 and J_2) for an isosceles triangle and an antisymmetric exchange, using the Hamiltonian shown below:

$$\hat{H} = -J_1(S_1S_2 + S_2S_3) - J_2(S_1S_3) - G\left(\hat{S}_1 \times \hat{S}_2 + \hat{S}_2 \times \hat{S}_3 + \hat{S}_1 \times \hat{S}_3\right) + \mu_B g H \sum_{i=1}^{3} \hat{S}_i \qquad (1)$$

The best-fit parameters obtained for the isotropic exchange interactions are J_1 = -193.5(6) cm^{-1} and J_2 = -205.5(3) cm^{-1} with an antisymmetric exchange parameter, $|G_z|$ = 28 cm^{-1} (solid line in Figure 3). These values are listed in Table 2, together with the magnetic parameters of selected molecular $[Cu_3\text{-}\mu_3OH]^{n+/-}$ pyrazolato complexes. The isotropic interaction values are strongly antiferromagnetic, being similar to those reported for other pyrazolato and triazolato triangular Cu_3OH complexes. The antisymmetric exchange interactions for triangular Cu^{II} hydroxido pyrazolato complexes have only been reported for two systems, **VAZCOR** ($|G_z|$ = -18.2 cm^{-1}) and **YIFGIG** ($|G_z|$ = -31.2 cm^{-1}) [17,35]. However, for complexes based on the triazolato ligand, there are more examples in the literature, with $|G_z|$ values between 17.5 and 44 cm^{-1} [24]. Thus, the isotropic and antisymmetric exchange interactions obtained for **1-Cu_3** are within the range observed for other triangular Cu^{II} hydroxy compounds (see Table 2).

Table 2. Selected examples of the magnetic and structural parameters of triangular Cu_3 pyrazolato systems of general formula, $[Cu_3(\mu_3\text{-}OH)(R\text{-}pz)_3(L)_3]^{n+/-}$.

CCDC Code	d(Cu^{II}-Cu^{II}) (Å)	Cu_3(plane)-OH (Å)	J(Cu^{II}···Cu^{II}) (cm^{-1})	g	zJ′ (cm^{-1})	$\|G_z\|$ (cm^{-1})	Ref
1-Cu_3	3.3740(8) 3.3574(8) 3.3702(9)	0.439	-193.5(6) -205.5(6)	2.09	-	28	This work
BOFLEP[#]	3.349(2) 3.239(2) 3.355(2)	0.580	-	-	-	-	[29]
DEFSEN	3.384(1) 3.2503(9) 3.2950(9)	0.567	-117.7 -90.3	2.047	-3.0	-	[22]
QISOW-a*	3.2559(7) 3.342(1) 3.2345(9)	0.713	-140	2.07	-	-	[23]
QISOW-b*	3.2045(6) 3.1837(8) 3.2007(9)	0.759	-109	2.07	-	-	[23]
QOPJIP	3.355(1) 3.386(1) 3.368(1)	0.466	-241.9	2.07	-23.0	-	[25]
SIJKOL	3.112(1)	0.658	-148	2.17	-	-	[33]

 doi:10.20944/preprints202305.1726.v1

	3.321(1) 3.321(1)		-23				
VAZCOR	3.1913(9) 3.391(1) 3.353(1)	0.599	-298 -257	2.12	-0.37	18.2	[35]
YIFGIG	3.3500(8) 3.2440(7) 3.3519(6)	0.521	-392 -278	2.09	-	31.2	[17]

[#] In this structure, the magnetic properties are qualitatively described, and no analytical interpretation was done.

Magneto-structural analysis on triangular systems was done using the experimental data of Table 2. According to the literature, two structural parameters have been selected to study their influence on the magnetic properties of these triangular systems. The first is the displacement of the μ_3-OH^- from the Cu_3 plane, where the magnetic interaction becomes more antiferromagnetic when the displacement is smaller [42]. The second corresponds to the Cu-(μ_3-X)-Cu angle, which seems to be sensitive to the magnetic coupling interaction. The magnetic coupling interaction is switched from ferromagnetic to antiferromagnetic when the angle varies from 76° to 120° [43]. The analysis of these structural parameters with the average magnetic exchange interactions shows that a general tendency is observed only with the displacement of the μ_3-OH^- from the Cu_3 plane (Figure 4).

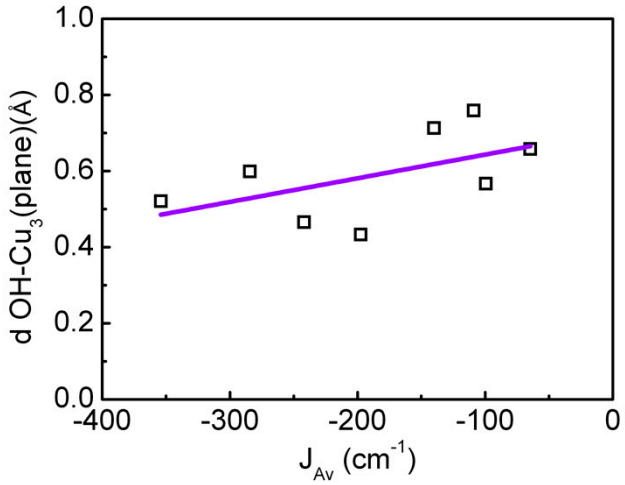

Figure 4. Relation between the displacement of the μ_3-OH^- from the Cu_3 plane and the average magnetic exchange interactions of triangular Cu_3 pyrazolato systems.

As mentioned in the Structural Analysis section, **1-Cu$_3$**, and **QOPJIP** are isostructural crystalline systems. According to the literature, the displacement of the μ_3-OH^- group from the Cu_3 plane influences the magnetic properties. This effect shows that a larger displacement causes a weaker antiferromagnetic interaction, which can be related to a weaker overlap of the magnetic orbitals of the Cu^{II} centers in the triangular system [44]. However, the smaller displacement observed for **1-Cu$_3$** (0.439 Å) than for **QOPJIP** (0.466 Å) suggests that **1-Cu$_3$** should present a stronger antiferromagnetic interaction between the copper centers than **QOPJIP**. However, the opposite phenomenon is observed (Figure 5).

Preprints.org (www.preprints.org) | NOT PEER-REVIEWED | Posted: 25 May 2023 doi:10.20944/preprints202305.1726.v1

A B

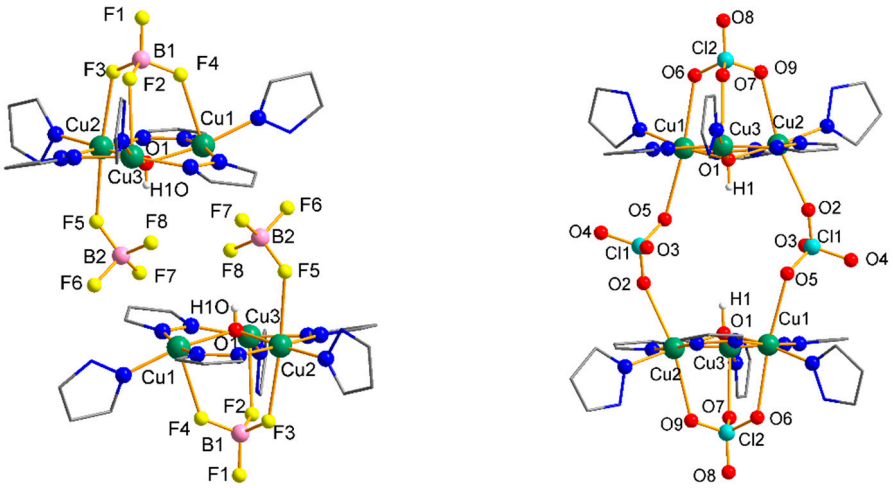

1-Cu$_3$
J_1 = -193.5(6) cm^{-1} and J_2 = -205.5(6) cm^{-1}
Cu1 and Cu3 SqP geometry
Cu2 Jahn-Teller O_h geometry
d(Cu$_3$ plane - μ_3-OH$^-$) = 0.439 Å

QOPJIP
J_1 = -241.9 cm^{-1}
Cu1 SqP geometry
Cu2 and Cu3 Jahn-Teller O_h geometry
d(Cu$_3$ plane - μ_3-OH$^-$) = 0.466 Å

Figure 5. A. Molecular structure of **1-Cu$_3$** and the magnetic exchange interaction obtained from the experimental data. **B**. Molecular structure of **QOPJIP** and the magnetic exchange interaction obtained from reference 25.

We have performed DFT calculations to rationalize the magnetic properties observed for **1-Cu$_3$** (see Materials and Methods section) [18]. The results were compared to a previously reported theoretical study of the magnetic properties of several μ_3-OH$^-$ bridged trinuclear Cu^{II} complexes [21]. The theoretical calculations for **1-Cu$_3$** were done under the same level of theory as for the study mentioned above. The geometrical array of the triangular unit for **1-Cu$_3$** permits to define three exchange pathways, with magnetic exchange interactions of J_1 = -94,9 cm^{-1}, J_2 = -87,7 cm$^{-1,}$ and J_3 = -98.6 cm^{-1}. For **QOPJIP**, previously reported DFT calculations also describe three exchange constants: J_1 = -118.3 cm^{-1}, J_2 = -106.0 cm$^{-1,}$ and J_3 = -120.6 cm^{-1}. The difference observed in the magnitude of the magnetic exchange interaction between the calculated and the one obtained by the fitting experimental data for both systems may be related to the so-called strong interaction limit, in which the weak interaction limit treatment of Noodleman would result in J-values generally twice as larger [18]. This difference could also be due because the experimental J values are obtained from bulk magnetic data that include other magnetic phenomena in the crystalline lattice. On the other hand, DFT calculations can isolate the magnetic phenomena for the molecular structure.

The DFT calculation of **1-Cu$_3$** was completely validated since the overlap parameters, together with their calculated magnetic exchange interactions, fit well on the plot of the J values of the seven studied complexes as a function of the square of the overlap depicted in the previous work of reference [21]. A linear relationship can be observed, as expected from the Kahn-Briat overlap model (Figure 6). These results permit us to infer that the μ_3-OH$^-$ bridged contributes to the exchange phenomenon, together with the other bridges. Finally, Mulliken spin density values were determined for four spin configurations. The obtained values for the Cu^{II} atoms are in 0.60-0.68 e$^-$ range, similar to those obtained for other similar Cu^{II} systems [18,21]. These results reflect that most of the electron spin density is located on the metal centers, and the rest of the spin density appears over the atoms of the first coordination sphere through a delocalization mechanism of the spin density. Figure S3 presents the spin density surfaces for the ferromagnetic solution S_T = 3/2 and three broken-symmetry

Preprints.org (www.preprints.org) | NOT PEER-REVIEWED | Posted: 25 May 2023 doi:10.20944/preprints202305.1726.v1

solutions $S_T = 1/2$ for **1-Cu$_3$**. It is possible to observe that no polarization mechanism of the spin density is observed for the corresponding second coordination spheres.

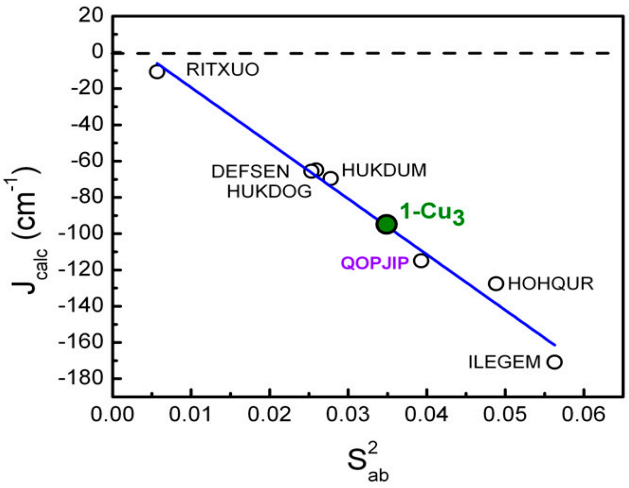

Figure 6. Dependence of the calculated J values with the square of the overlap integral of the magnetic orbitals. Adapted from Ref. [28], Copyright (2013), with permission from Springer.

Finally, from all the results discussed above, it is possible to conclude that both compounds, **1-Cu$_3$** and **QOPJIP**, have a similar trinuclear structure with a μ_3-OH^- and μ_2-pz^- bridges and both systems show a tetrahedral anion with a μ_3 coordination mode ($[BF_4]^-$ and $[ClO_4]^-$). The average DFT calculated J values for **1-Cu$_3$**, and **QOPJIP** are -93.7 and -114.9 cm^{-1}, respectively. The displacement of the μ_3-OH^- group from the plane of the three copper atoms is smaller for **1-Cu$_3$** (0.439 Å) than for **QOPJIP** (0.466 Å); thus, the first system should have stronger antiferromagnetic interactions, in contrast with the experimental values. These results suggest that the μ_3-ClO_4^- anion is not an innocent ligand and favors an antiferromagnetic exchange between the Cu^{II} centers, resulting in a stronger antiferromagnetic coupling in **QOPJIP**.

3. Materials and Methods

Synthesis of $[Cu_3(\mu_3\text{-}OH)(pz)_3(Hpz)_3][BF_4]_2$ (1-Cu$_3$)

$Cu(BF_4)_2{\cdot}H_2O$ (765.5 mg, 3 mmol) was dissolved in 20 mL of methanol. Then, a solution of pyrazole (204.2 mg, 3 mmol) and dimethylamine (135.2 mg, 3 mmol) in 15 mL of methanol was added to the first solution. After adding the second solution, the color changes from light blue to greenish blue in the final solution. Greenish blue crystals of **1-Cu$_3$**, suitable for X-ray diffraction, were obtained within three days by slow evaporation of the filtered solution at room temperature. Elemental analysis (Found: C, 27.9 %; N, 19.5 %; H, 3.2 %. Calc. for $Cu_3C_{18}H_{22}N_{12}OB_2F_8$: C, 27.5 %; N, 21.4 %; H, 2.8 %). Elemental ratio estimated by electron probe microanalysis (EPMA): (Exp.) Theo. Cu : F = (2.89)3 : (8.03)8. ES-MS in positive mode (acetonitrile) shows the existence of only $[Cu_3(\mu_3\text{-}OH)]^{2+}$ unit, confirmed by mass-spectrometry. The experiments show the existence of the $\{[Cu_3(\mu_3\text{-}OH)(pz)_3(Hpz)_3][BF_4]\}^+$ (m/Z = 700); $\{[Cu_3(\mu_3\text{-}OH)(pz)_3(Hpz)_3]+1e^-\}^+$ (m/Z = 613); $\{[Cu_3(\mu_3\text{-}OH)(pz)_3(Hpz)_2]+1e^-\}^+$ (m/Z = 544); $\{[Cu_3(\mu_3\text{-}OH)(pz)_3(Hpz)_1]\ ]+1e^-\}^+$ (m/Z = 476); $\{[Cu_3(\mu_3\text{-}OH)(pz)_3\}^+$ (m/Z = 408). See Figure S1. IR data (KBr, ν_{max}/cm^{-1}) 3400m [ν(NH)], 3137w [$\nu(\mu_3\text{-}OH^-)$], 1650w, and 1200w [ν_{as}(CN aromatic)]. See Figure S2.

Physical Characterization

Fourier transform infrared spectroscopy (FTIR) was performed using a NICOLET 5700 (Thermofisher Scientific, Waltham, MA, USA) in the range 4000-650 cm^{-1}. Elemental analysis (C, N, H) was performed by microanalytical procedures using an EA 1108 elemental analyzer (CE

 doi:10.20944/preprints202305.1726.v1

Instruments, Wigan, UK). Electrospray ionization mass spectrometry (ESI-MS) studies of **1-Cu$_3$** were performed with a QTOF Premier instrument with an orthogonal Z-spray-electrospray interface (Waters, Manchester, UK). A capillary voltage of 3.5 kV was used in the positive scan mode, and the cone voltage was set to 10 V to control the extent of fragmentation.

X-ray Diffraction

A single crystal of compound **1-Cu$_3$** was mounted on a glass fiber, using a hydrocarbon oil to coat the crystal, and then transferred directly to the cold nitrogen stream for data collection. X-ray data were collected at 120 K on a Supernova diffractometer (Rigaku, Austin, TX, USA) equipped with a graphite-monochromated Enhance (Mo) X-ray Source (λ = 0.71073 Å). The program CrysAlisPro, Oxford Diffraction Ltd., was used for unit cell determination and data reduction. Empirical absorption correction was performed using spherical harmonics, implemented in the SCALE3 ABSPACK scaling algorithm. The structure was solved with the ShelXT structure solution program [45] and refined with the SHELXL-2018 program [46] using Olex 2 [47]. Non-hydrogen atoms were refined anisotropically, and hydrogen atoms were placed in calculated positions that were refined using idealized geometries (riding model). A summary of the data collection and structure refinements is provided in Table S1. CCDC-**2174487 (1-Cu$_3$)** contains the supplementary crystallographic data for this paper. These data can be obtained free of charge from The Cambridge Crystallographic Data Center via www.ccdc.cam.ac.uk/data_request/cif.

Magnetic Susceptibility Measurements

Variable temperature susceptibility measurements were carried out for **1-Cu$_3$** in the temperature range of 2-300 K with an applied magnetic field of 100 mT on a ground polycrystalline sample (with a mass of 37.64 mg**)** with a Quantum Design (San Diego, CA, USA) MPMS XL-5 SQUID magnetometer. The susceptibility data were corrected for the diamagnetic contributions of the sample using Pascal´s constants [48]. Isothermal magnetization measurements were made between 0 and 5 T at 2 K.

DFT Calculations of the Magnetic Properties

Spin-unrestricted calculations under the Density Functional Theory approach were done using the hybrid B3LYP functional [49,50] and a triple-ζ all-electron basis set for all atoms in all the calculations [51]. A guess function was generated using the Jaguar 5.5 code [52]. Total energy calculations were performed with the Gaussian09 code [53], using the quadratic convergence approach with a convergence criterion of 10^{-7} a.u. Mulliken spin densities were obtained from the Single Point calculations using Gaussian09.

The Heisenberg-Dirac-van Vleck spin Hamiltonian was used to describe the exchange coupling in the trinuclear complex is $\hat{H} = -\sum_{i>j} J_{ij} S_i S_j$; where S_i and S_j are the spin operators of the paramagnetic centers of the compound. The J_i parameters are the magnetic coupling constants between neighboring centers with unpaired electrons. Four different spin distributions (three antiferromagnetic and one ferromagnetic) for the system were calculated, and the obtained energies permit to evaluate the magnetic exchange constants of the system.

Utilizing the non-projected energy of the broken symmetry solution as the energy of the low spin state within the DFT methodology gives good results because it avoids the cancellation of the non-dynamic correlation effects, as has been stated in studies carried out by Ruiz et al. Thus, the J value is obtained using the non-projected method [54,55].

4. Conclusions

A new trinuclear cationic $[Cu_3\text{-}\mu_3OH]^{n+}$ complex based on the pyrazolato ligand has been obtained, $[Cu_3(\mu_3\text{-}OH)(pz)_3(Hpz)_3][BF_4]_2$ (**1-Cu$_3$**). The triangular complex presents the $[BF_4]^-$ as counter-anion and is isostructural with the **QOPJIP** system. Nevertheless, the smaller size of the BF_4^-

anion in **1-Cu$_3$**, compared to the ClO_4^- anion in **QOPJIP**, prevents the connection of the triangular units in **1-Cu$_3$**, in contrast to what is observed for the isostructural complex **QOPJIP.**

The magnetic data shows that strong antiferromagnetic interactions, together with antisymmetric interactions, exist in the triangular unit. The analysis of the experimental data and theoretical DFT results lead to the conclusion that there is a correlation between the displacement of the μ_3-OH^- from the Cu_3 plane and the magnetic exchange interactions of the triangular Cu_3 pyrazolato systems. However, the presence of other bridging organic ligands also plays a role in the magnetic exchange. These features affect the overlap of the magnetic orbitals according to the Khan-Briat model, suggesting that a strong overlap of magnetic orbitals exists in these systems.

The differences in the magnetic properties between **1-Cu$_3$** and **QOPJIP** were analyzed and rationalized, showing that the different structural parameters, such as the displacement of the μ_3-OH^- from the Cu_3 plane, the nature of the bridging organic ligands and also the size of the counter-anion affect the overall magnetic properties of these systems.

Supplementary Materials: The following supporting information can be downloaded at the website of this paper posted on Preprints.org, **Figure S1**. Electrospray-Mass Spectrometry **1-Cu$_3$** measurements in the positive mode with the different simulated fragments patterns **Figure S2.** FTIR Spectra of **1-Cu$_3$**. **Figure S3**. Spin density surfaces for **1-Cu$_3$** of the antiferromagnetic configurations and the ferromagnetic one. **Table S1**. Crystal data and structure refinement for **1-Cu$_3$**. **Table S2**. Fractional Atomic Coordinates and Equivalent Isotropic Displacement Parameters for **1-Cu$_3$**. **Table S3**. Anisotropic Displacement Parameters for **1-Cu$_3$**. **Table S4**. Bond Lengths for **1-Cu$_3$**. **Table S5.** Bond Angles for **1-Cu$_3$. Table S6.** Hydrogen Atom Coordinates and Isotropic Displacement Parameters for **1-Cu$_3$**.

Author Contributions: Conceptualization, W.C-M., D.V-Y, E.S. and C.J.G-G.; formal analysis, W.C-M. and P.H-I..; investigation, W.C-M., P.H-I. and C.J.G-G.; writing-original draft preparation, W.C-M., P.H-I. and V.P.-G.; writing-review and editing, W.C-M., D.V-Y, E.S., V.P.-G. and C.J.G-G.. All authors have read and agreed to the published this version of the manuscript.

Funding: Authors acknowledge Financiamiento Basal Program AFB220001 for partial financial support. Powered@NLHPC: This research was partially supported by the supercomputing infrastructure of the NLHPC (ECM-02), Center for Mathematical Modelling CMM, Universidad de Chile. The authors acknowledge CONICYT-FONDEQUIP/EQM130086-EQM140060. This work was done under partial support of the Chilean-French International Research Program "IRP-CoopIC". This study forms part of the Advanced Materials program and was supported by MCIN with funding from European Union Next Generation EU (PRTR-C17.I1) and the Generalitat Valenciana (project MFA-2022-057). We also thank the Generalidad Valenciana (Prometeo/2019/076) and the project PID2021-125907NB-I00, financed by MCIN/AEI/10.13039/501100011033/FEDER, UE, for financial support.

Acknowledgments: The authors thank Dr. Guillermo Mínguez Espallargas from Instituto de Ciencia Molecular (ICMol), Universitat de Valencia, for performing the single crystal XRD and for fruitful discussion on the crystallographic and structural data.

Conflicts of Interest: The authors declare no conflict of interest.

References

1. Scatena, R.; Massignani, S.; Lanza, A.E.; Zorzi, F.; Monari, M.; Nestola, F.; Pettinari, C.; Pandolfo, L. Synthesis of Coordination Polymers and Discrete Complexes from the Reaction of Copper(II) Carboxylates with Pyrazole: Role of Carboxylates Basicity. *Cryst. Growth Des.* **2022**, *22*, 1032–1044, doi:10.1021/acs.cgd.1c00861.
2. Di Nicola, C.; Karabach, Y.Y.; Kirillov, A.M.; Monari, M.; Pandolfo, L.; Pettinari, C.; Pombeiro, A.J.L. Supramolecular assemblies of trinuclear triangular copper(II) secondary building units through hydrogen bonds. Generation of different metal-organic frameworks, valuable catalysts for peroxidative oxidation of alkanes. *Inorg. Chem.* **2007**, *46*, 221–30, doi:10.1021/ic061595n.
3. Angaridis, P.A.; Baran, P.; Boc˘a, R.; Cervantes-Lee, F.; Haase, W.; Mezei, G.; Raptis, R.G.; Werner, R. Synthesis and Structural Characterization of Trinuclear Cu^{II} –Pyrazolato Complexes Containing μ_3-OH, μ_3-O, and μ_3-Cl Ligands. Magnetic Susceptibility Study of $[PPN]_2[(\mu_3\text{-}O)Cu_3(\mu\text{-}pz)_3Cl_3]$. *Inorg. Chem.* **2002**, *41*, 2219–2228, doi:10.1021/ic010670l.
4. Bala, S.; Bhattacharya, S.; Goswami, A.; Adhikary, A.; Konar, S.; Mondal, R. Designing functional metal-organic frameworks by imparting a hexanuclear copper-based secondary building unit specific properties:

Structural correlation with magnetic and photocatalytic activity. *Cryst. Growth Des.* **2014**, *14*, 6391–6398, doi:10.1021/cg501226v.

5. Condello, F.; Garau, F.; Lanza, A.; Monari, M.; Nestola, F.; Pandolfo, L.; Pettinari, C. Synthesis and structural characterizations of new coordination polymers generated by the interaction between the trinuclear triangular SBU $[Cu_3(\mu_3\text{-}OH)(\mu\text{-}pz)_3]^{2+}$ and 4,4'-Bipyridine. 3°. *Cryst. Growth Des.* **2015**, *15*, 4854–4862, doi:10.1021/acs.cgd.5b00661.
6. Rivera-Carrillo, M.; Chakraborty, I.; Raptis, R.G. Systematic synthesis of a metal organic framework based on triangular $Cu_3(\mu_3\text{-}OH)$ secondary building units: From a 0-D complex to a 1-D chain and a 3-D lattice. *Cryst. Growth Des.* **2010**, *10*, 2606–2612, doi:10.1021/cg100060p.
7. Trif, M.; Troiani, F.; Stepanenko, D.; Loss, D. Spin-electric coupling in molecular magnets. *Phys. Rev. Lett.* **2008**, *101*, 1–4, doi:10.1103/PhysRevLett.101.217201.
8. Troiani, F.; Stepanenko, D.; Loss, D. Hyperfine-induced decoherence in triangular spin-cluster qubits. *Phys. Rev. B - Condens. Matter Mater. Phys.* **2012**, *86*, 161409, doi:10.1103/PhysRevB.86.161409.
9. Belinsky, M.I. Spin Chirality of Cu_3 and V_3 Nanomagnets. 1. Rotation Behavior of Vector Chirality, Scalar Chirality, and Magnetization in the Rotating Magnetic Field, Magnetochiral Correlations. *Inorg. Chem.* **2016**, *55*, 4078–4090, doi:10.1021/acs.inorgchem.5b02202.
10. Belinsky, M.I. Spin Chirality of Cu_3 and V_3 Nanomagnets. 2. Frustration, Temperature, and Distortion Dependence of Spin Chiralities and Magnetization in the Rotating and Tilted Magnetic Fields. *Inorg. Chem.* **2016**, *55*, 4091–4109, doi:10.1021/acs.inorgchem.5b02204.
11. Kintzel, B.; Böhme, M.; Liu, J.; Burkhardt, A.; Mrozek, J.; Buchholz, A.; Ardavan, A.; Plass, W. Molecular electronic spin qubits from a spin-frustrated trinuclear copper complex. *Chem. Commun.* **2018**, *54*, 12934–12937, doi:10.1039/c8cc06741d.
12. Boudalis, A.K. Half-Integer Spin Triangles: Old Dogs, New Tricks. *Chem. – A Eur. J.* **2021**, *27*, 7022–7042, doi:10.1002/chem.202004919.
13. Spielberg, E.T.; Gilb, A.; Plaul, D.; Geibig, D.; Hornig, D.; Schuch, D.; Buchholz, A.; Ardavan, A.; Plass, W. A Spin-Frustrated Trinuclear Copper Complex Based on Triaminoguanidine with an Energetically Well-Separated Degenerate Ground State. *Inorg. Chem.* **2015**, *54*, 3432–3438, doi:10.1021/ic503095t.
14. Sowrey, F.E.; Tilford, C.; Wocadlo, S.; Anson, C.E.; Powell, A.K.; Bennington, S.M.; Montfrooij, W.; Jayasooriya, U. a.; Cannon, R.D. Spin frustration and concealed asymmetry: structure and magnetic spectrum of $[Fe_3O(O_2CPh)_6(py)_3]ClO_4 \cdot py$†. *J. Chem. Soc. Dalt. Trans.* **2001**, *6*, 862–866, doi:10.1039/b008121n.
15. Tsukerblat, B.S.; Belinskii, M.I.; Fainzil´berg, V.E. Magnetochemistry and Spectroscopy of Transition Metals Exchange Clusters. *Sov. Sci. Rev. B Chem.* **1987**, *9*, 337–481.
16. Toader, A.M.; Buta, M.C.; Cimpoesu, F.; Toma, A.-I.; Zalaru, C.M.; Cinteza, L.O.; Ferbinteanu, M. New Syntheses, Analytic Spin Hamiltonians, Structural and Computational Characterization for a Series of Tri-, Hexa- and Hepta-Nuclear Copper (II) Complexes with Prototypic Patterns. *Chemistry (Easton).* **2021**, *3*, 411–439, doi:10.3390/chemistry3010031.
17. Mathivathanan, L.; Boudalis, A.K.; Turek, P.; Pissas, M.; Sanakis, Y.; Raptis, R.G. Interactions between H-bonded $[Cu^{II}_3(\mu_3\text{-}OH)]$ triangles; A combined magnetic susceptibility and EPR study. *Phys. Chem. Chem. Phys.* **2018**, *20*, 17234–17244, doi:10.1039/c8cp02643b.
18. Shi, K.; Mathivathanan, L.; Herchel, R.; Boudalis, A.K.; Raptis, R.G. Supramolecular Assemblies of Trinuclear Copper(II)-Pyrazolato Units: A Structural, Magnetic and EPR Study. *Chemistry (Easton).* **2020**, *2*, 626–644, doi:10.3390/chemistry2030039.
19. Mezei, G.; Raptis, R.G.; Telser, J. Trinuclear, antiferromagnetically coupled Cu^{II} complex with an EPR spectrum of mononuclear Cu^{II}: Effect of alcoholic solvents. *Inorg. Chem.* **2006**, *45*, 8841–8843, doi:10.1021/ic061186r.
20. Mukherjee, P.; Drew, M.G.B.; Estrader, M.; Diaz, C.; Ghosh, A. Influence of counter anions on the structures and magnetic properties of trinuclear Cu(II) complexes containing a μ_3-OH core and Schiff base ligands. *Inorganica Chim. Acta* **2008**, *361*, 161–172, doi:10.1016/j.ica.2007.06.037.
21. Cañon-Mancisidor, W.; Spodine, E.; Paredes-Garcia, V.; Venegas-Yazigi, D. Theoretical description of the magnetic properties of μ_3-hydroxo bridged trinuclear copper(II) complexes. *J. Mol. Model.* **2013**, *19*, 2835–44, doi:10.1007/s00894-012-1696-5.
22. Zhou, J.-H.; Liu, Z.; Li, Y.-Z.; Song, Y.; Chen, X.-T.; You, X.-Z. Synthesis, structures and magnetic properties of two copper(II) complexes with pyrazole and pivalate ligands. *J. Coord. Chem.* **2006**, *59*, 147–156, doi:10.1080/00958970500266206.
23. Davydenko, Y.M.; Demeshko, S.; Pavlenko, V. a.; Dechert, S.; Meyer, F.; Fritsky, I.O. Synthesis, Crystal Structure, Spectroscopic and Magnetically Study of Two Copper(II) Complexes with Pyrazole Ligand. *Zeitschrift für Anorg. und Allg. Chemie* **2013**, *639*, 1472–1476, doi:10.1002/zaac.201300078.
24. Ferrer, S.; Lloret, F.; Pardo, E.; Clemente-Juan, J.M.; Liu-González, M.; García-Granda, S. Antisymmetric Exchange in Triangular Tricopper(II) Complexes: Correlation among Structural, Magnetic, and Electron Paramagnetic Resonance Parameters. *Inorg. Chem.* **2012**, *51*, 985–1001, doi:10.1021/ic2020034.

25. Zhou, Q.-J.; Liu, Y.-Z.; Wang, R.-L.; Fu, J.-W.; Xu, J.-Y.; Lou, J.-S. Synthesis, crystal structure and magnetic properties of a trinuclear Cu(II)-pyrazolate complex containing μ_3-OH. *J. Coord. Chem.* **2009**, *62*, 311–318, doi:10.1080/00958970802238531.
26. Shi, K.; Mathivathanan, L.; Boudalis, A.K.; Turek, P.; Chakraborty, I.; Raptis, R.G. Nitrite Reduction by Trinuclear Copper Pyrazolate Complexes: An Example of a Catalytic, Synthetic Polynuclear NO Releasing System. *Inorg. Chem.* **2019**, *58*, 7537–7544, doi:10.1021/acs.inorgchem.9b00748.
27. Massignani, S.; Scatena, R.; Lanza, A.; Monari, M.; Condello, F.; Nestola, F.; Pettinari, C.; Zorzi, F.; Pandolfo, L. Coordination polymers from mild condition reactions of copper(II) carboxylates with pyrazole (Hpz). Influence of carboxylate basicity on the self-assembly of the $[Cu_3(\mu_3\text{-}OH)(\mu\text{-}pz)_3]^{2+}$ secondary building unit. *Inorganica Chim. Acta* **2017**, *455*, 618–626, doi:10.1016/j.ica.2016.05.009.
28. Ahmed, B.M.; Mezei, G. From ordinary to extraordinary: Insights into the formation mechanism and pH-dependent assembly/disassembly of nanojars. *Inorg. Chem.* **2016**, *55*, 7717–7728, doi:10.1021/acs.inorgchem.6b01172.
29. Alsalme, A.; Ghazzali, M.; Khan, R.A.; Al-Farhan, K.; Reedijk, J. A novel trinuclear μ_3-hydroxido-bridged Cu(II) compound; A molecular cluster, stabilized by hydrogen bonding, bridging pyrazolates, terminal pyrazoles, water and nitrate anions. *Polyhedron* **2014**, *75*, 64–67, doi:10.1016/j.poly.2014.03.017.
30. Di Nicola, C.; Garau, F.; Gazzano, M.; Monari, M.; Pandolfo, L.; Pettinari, C.; Pettinari, R. Reactions of a coordination polymer based on the triangular cluster $[Cu_3(\mu_3\text{-}OH)(\mu\text{-}pz)_3]^{2+}$ with strong acids. Crystal structure and supramolecular assemblies of new mono-, tri-, and hexanuclear complexes and coordination polymers. *Cryst. Growth Des.* **2010**, *10*, 3120–3131, doi:10.1021/cg1002397.
31. Casarin, M.; Cingolani, A.; Di Nicola, C.; Falcomer, D.; Monari, M.; Pandolfo, L.; Pettinari, C. The Different Supramolecular Arrangements of the Triangular $[Cu_3(\mu_3\text{-}OH)(\mu\text{-}pz)_3]^{2+}$ (pz = Pyrazolate) Secondary Building Units. Synthesis of a Coordination Polymer with Permanent Hexagonal Channels. *Cryst. Growth Des.* **2007**, *7*, 676–685, doi:10.1021/cg060501h.
32. Vynohradov, O.S.; Pavlenko, V.A.; Fritsky, I.O.; Gural'skiy, I.A.; Shova, S. Synthesis and Crystal Structure of Copper(II) 9-Azametallacrowns-3 with 4-Iodopyrazole. *Russ. J. Inorg. Chem.* **2020**, *65*, 1481–1488, doi:10.1134/S0036023620100228.
33. Angaroni, M.; Ardizzoia, G.A.; Beringhelli, T.; La Monica, G.; Gatteschi, D.; Masciocchi, N.; Moret, M. Oxidation reaction of $[\{Cu(Hpz)_2Cl\}_2]$(Hpz = pyrazole): synthesis of the trinuclear copper(II) hydroxo complexes $[Cu_3(OH)(pz)_3(Hpz)_2Cl_2]\cdot$solv (solv = H_2O or tetrahydrofuran). Formation, magnetic properties, and X-ray crystal structure of $[Cu_3(OH)(pz)_3(py)_2Cl_2]\cdot$py (py = pyridine). *J. Chem. Soc. Dalt. Trans.* **1990**, 3305–3309, doi:10.1039/DT9900003305.
34. Liu, X.; Nie, Y.; Tang, Q.; Tian, A.; Hu, Z.; Yan, J.; Zhang, S. Pyrazole-based trinuclear and mononuclear complexes: synthesis, characterization, DNA interactions and cytotoxicity studies. *Transit. Met. Chem.* **2021**, *46*, 481–494, doi:10.1007/s11243-021-00466-4.
35. Boudalis, A.K.; Rogez, G.; Heinrich, B.; Raptis, R.G.; Turek, P. Towards ionic liquids with tailored magnetic properties: Bmim+ salts of ferro- and antiferromagnetic Cu^{II}_3 triangles. *Dalt. Trans.* **2017**, *46*, 12263–12273, doi:10.1039/c7dt02472j.
36. Razali, M.R.; Urbatsch, A.; Deacon, G.B.; Batten, S.R. Transition metal complexes of the small cyano anion dicyanonitromethanide $[C(CN)_2(NO_2)]^-$ Dedicated to George Christou on the occasion of his 60th birthday. *Polyhedron* **2013**, *64*, 352–364, doi:10.1016/j.poly.2013.06.018.
37. Rivera-Carrillo, M.; Chakraborty, I.; Mezei, G.; Webster, R.D.; Raptis, R.G. Tuning of the [Cu3(μ-O)]4+/5+ redox couple: Spectroscopic evidence of charge delocalization in the mixed-valent $[Cu_3(\mu\text{-}O)]^{5+}$ species. *Inorg. Chem.* **2008**, *47*, 7644–7650, doi:10.1021/ic800531y.
38. Lang, J.; Hewer, J.M.; Meyer, J.; Schuchmann, J.; van Wüllen, C.; Niedner-Schatteburg, G. Magnetostructural correlation in isolated trinuclear iron(III) oxo acetate complexes. *Phys. Chem. Chem. Phys.* **2018**, *20*, 16673–16685, doi:10.1039/C7CP07549A.
39. Antkowiak, M.; Kamieniarz, G.; Florek, W. Comment on "Magnetostructural correlations in isolated trinuclear iron(III) oxo acetate complexes" by J. Lang, J. M. Hewer, J. Meyer, J. Schuchmann, C. van Wüllen and G. Niedner-Schatteburg,: Phys. Chem. Chem. Phys., 2018, 20, 16673. *Phys. Chem. Chem. Phys.* **2019**, *21*, 504, doi:10.1039/c8cp04691c.
40. van Wüllen, C.; Lang, J.; Niedner-Schatteburg, G. Reply to the 'Comment on "Magnetostructural correlations in isolated trinuclear iron(III) oxo acetate complexes"' by M. Antkowiak, G. Kamieniarz and W. Florek, *Phys. Chem. Chem. Phys.* , 2018, 20, DOI: 10.1039/C8CP04691C. *Phys. Chem. Chem. Phys.* **2019**, *21*, 505–506, doi:10.1039/C8CP05926H.
41. Chilton, N.F.; Anderson, R.P.; Turner, L.D.; Soncini, A.; Murray, K.S. PHI: A powerful new program for the analysis of anisotropic monomeric and exchange-coupled polynuclear d- and f-block complexes. *J. Comput. Chem.* **2013**, *34*, 1164–1175, doi:10.1002/jcc.23234.
42. Afrati, T.; Dendrinou-Samara, C.; Raptopoulou, C.; Terzis, A.; Tangoulis, V.; Tsipis, A.; Kessissoglou, D.P. Experimental and theoretical study of the antisymmetric magnetic behavior of copper inverse-9-metallacrown-3 compounds. *Inorg. Chem.* **2008**, *47*, 7545–7555, doi:10.1021/ic8003257.

43. Wang, L.-L.; Sun, Y.-M.; Yu, Z.-Y.; Qi, Z.-N.; Liu, C.-B. Theoretical Investigation on Triagonal Symmetry Copper Trimers: Magneto-Structural Correlation and Spin Frustration. *J. Phys. Chem. A* **2009**, *113*, 10534–10539, doi:10.1021/jp9045897.
44. Yoon, J.; Solomon, E.I. Ground-state electronic and magnetic properties of a μ_3-oxo-bridged trinuclear Cu(II) complex: correlation to the native intermediate of the multicopper oxidases. *Inorg. Chem.* **2005**, *44*, 8076–86, doi:10.1021/ic0507870.
45. Sheldrick, G.M. SHELXT – Integrated space-group and crystal-structure determination. *Acta Crystallogr. Sect. A Found. Adv.* **2015**, *71*, 3–8, doi:10.1107/S2053273314026370.
46. Sheldrick, G.M. Crystal structure refinement with SHELXL. *Acta Crystallogr. Sect. C Struct. Chem.* **2015**, *71*, 3–8, doi:10.1107/S2053229614024218.
47. Dolomanov, O. V.; Bourhis, L.J.; Gildea, R.J.; Howard, J.A.K.; Puschmann, H. OLEX2 : a complete structure solution, refinement and analysis program. *J. Appl. Crystallogr.* **2009**, *42*, 339–341, doi:10.1107/S0021889808042726.
48. Bain, G.A.; Berry, J.F. Diamagnetic Corrections and Pascal's Constants. *J. Chem. Educ.* **2008**, *85*, 532–536.
49. Becke, A.D. Density-functional thermochemistry. III. The role of exact exchange. *J. Chem. Phys.* **1993**, *98*, 5648–5652.
50. Yanai, T.; Tew, D.P.; Handy, N.C. A new hybrid exchange-correlation functional using the Coulomb-attenuating method (CAM-B3LYP). *Chem. Phys. Lett.* **2004**, *393*, 51–57, doi:10.1016/j.cplett.2004.06.011.
51. Schafer, A.; Huber, C.; Ahlrichs, R. Fully optimized contracted quality for atoms Li to Kr Gaussian basis sets of triple zeta valence quality for atoms Li to Kr. *J. Chem. Phys.* **1994**, *100*, 5829–5835.
52. Jaguar Jaguar 5.5. *version 5.5; Schrödinger, LLC Portland, OR* **2003**.
53. Frisch, M.J.; Trucks, G.W.; Schlegel, H.B.; Scuseria, G.E.; Robb, M.A.; Cheeseman, J.R.; Montgomery, J.A.; Vreven, T.; Kudin, K.N.; Burant, J.C.; et al. G09. *Gaussian 09 (Revision D.2), Gaussian, Inc., Pittsburgh, PA* 2009.
54. Ruiz, E.; Alvarez, S.; Cano, J.; Polo, V. About the calculation of exchange coupling constants using density-functional theory: the role of the self-interaction error. *J. Chem. Phys.* **2005**, *123*, 164110, doi:10.1063/1.2085171.
55. Ruiz, E. Theoretical Study of the Exchange Coupling in Large Polynuclear Transition Metal Complexes Using DFT Methods. *Struct. Bond.* **2004**, *113*, 71–102, doi:10.1007/b97942.